Generalized partition function zeros of 1D spin models and their critical behavior at edge singularities

2010 J. Phys. A: Math. Theor. 43 255002

(http://iopscience.iop.org/1751-8121/43/25/255002)

J. Phys. A: Math. Theor. **43** (2010) 255002 (20pp) doi:10.1088/1751-8113/43/25/255002

Generalized partition function zeros of 1D spin models and their critical behavior at edge singularities

D Dalmazi and F L Sá

UNESP—Univ. Estadual Paulista, Campus de Guaratinguetá, DFQ, Av. Dr. Ariberto P. da Cunha, 333, CEP 12516-410 Guaratinguetá, São Paulo, Brazil

E-mail: dalmazi@feg.unesp.br and ferlopessa@yahoo.com.br

Received 7 January 2010, in final form 15 April 2010
Published 28 May 2010
Online at stacks.iop.org/JPhysA/43/255002

Abstract

Here we study the partition function zeros of the one-dimensional Blume–Emery–Griffiths model close to their edge singularities. The model contains four couplings (H, J, Δ, K) including the magnetic field H and the Ising coupling J. We assume that only one of the three couplings (J, Δ, K) is complex and the magnetic field is real. The generalized zeros z_i tend to form continuous curves on the complex z-plane in the thermodynamic limit. The linear density at the edges z_E diverges usually with $\rho(z) \sim |z - z_E|^{\sigma}$ and $\sigma = -1/2$. However, as in the case of complex magnetic fields (Yang–Lee edge singularity), if we have a triple degeneracy of the transfer matrix eigenvalues a new critical behavior with $\sigma = -2/3$ can appear as we prove here explicitly for the cases where either Δ or K is complex. Our proof applies for a general three-state spin model with short-range interactions. The Fisher zeros (complex J) are more involved; in practice, we have not been able to find an explicit example with $\sigma = -2/3$ as far as the other couplings (H, Δ, K) are kept as real numbers. Our results are supported by numerical computations of zeros. We show that it is absolutely necessary to have a non-vanishing magnetic field for a new critical behavior. The appearance of $\sigma = -2/3$ at the edge closest to the positive real axis indicates its possible relevance for tricritical phenomena in higher-dimensional spin models.

PACS numbers: 05.70.Jk, 05.50.+q, 05.70.Fh

(Some figures in this article are in colour only in the electronic version)

1. Introduction

One possible way of studying critical phenomena and phase transitions in a physical system is to calculate its partition function, rewrite it as a polynomial on some variable z and calculate its zeros z_i on the complex z-plane. The zeros correspond to branch points of the free energy. This approach has been started in [1] and since then has found an increasing number of applications in different areas of physics, see the review work [2]. The location and density of the zeros give precise information about the critical values of the physical parameters and the order of the phase transition, respectively. Even when a physical phase transition is absent, like the case of spin models with short-range interaction in $d = 1$ dimension, or in $d \geqslant 2$ above the critical temperature ($T > T_{\mathrm{cr}}$), the partition function zeros display a universal behavior [3]. In the thermodynamic limit, the zeros z_i usually tend to form continuous curves on the complex z-plane. At the edges (z_E) of those curves, the linear density of zeros $\rho(z)$ diverges with a critical exponent σ, i.e. $\rho(z) \sim |z - z_E|^\sigma$ with $\sigma < 0$. The exponent σ is apparently universal and only depends on the dimension d. This unusual critical phenomenon is described by a nonunitary local field theory with a $\mathrm{i}\,\varphi^3$ interaction term, see [3]. This is the case, at least, of complex magnetic field (H) zeros where $z = \mathrm{e}^{H/k_B T}$.

In $d = 2$ dimensions, the $\mathrm{i}\,\varphi^3$ scalar theory becomes at the critical point a conformal field theory corresponding to the nonunitary minimal model $(p, q) = (2, 5)$, see [4]. In this minimal model there is only one relevant physical field $\phi_{1,2}$ or its equivalent $\phi_{1,3}$, with conformal weight $\Delta_{1,2} = \Delta_{1,3} = -1/5$. From $\Delta_{1,2}$ one [4] obtains $\sigma = -1/6$. Such a result is in accordance with the numerical calculations based on low-temperature and high-field series expansions of [5] and numerical computations of the partition function zeros, with the help of finite-size scaling (FSS) relations, of [6]. Remarkably, since the density of zeros $\rho(H)$ (for complex magnetic fields H) can be extracted from the discontinuity of the magnetization, it is possible to access $\rho(H)$ close to the edge singularity H_E from experimental magnetization data as in [7]. Those experimental data [7] are also consistent with $\sigma = -1/6$.

The exponent σ is related to the magnetic scaling exponent y_H via $\sigma = (d - y_H)/y_H$. In $d = 2$, we have, above the critical temperature, $y_H = 12/5$ ($\sigma = -1/6$). In $d = 1$, for $T > 0$, the usual result is $y_H = 2$ ($\sigma = -1/2$) which can be proved analytically for several models like the spin-1/2 Ising model (second reference of [1]), the Q-state Potts model with $Q > 0$ except at $Q = 1$ [8], the Blume–Capel (BC) model [9] and the Blume–Emery–Griffiths (BEG) model [10]. For the last model, we have made use in [10] of FSS relations derived in [11] and assumed that there are no triple degeneracy of the transfer matrix eigenvalues. There are also earlier works [12–14] with model-independent arguments in favor of $\sigma = -1/2$.

Although the most studied case of partition function zeros corresponds to complex magnetic fields, at real temperatures, there are several works on complex temperature zeros, at real magnetic fields, the so-called Fisher zeros [15]. They are studied on the complex z-plane with $z = \mathrm{e}^{-J/k_B T}$ where J is the Ising coupling, see e.g. [8, 9, 11, 15–17]. There are also works [18, 19] where both H and J are complex. It turns out, as a general rule, that the Fisher zeros are more sensitive to the details of the lattice and have a more involved distribution, see for instance [20]. However, in many cases they also tend to be continuous curves in the thermodynamic limit, see e.g. [21], and have a universal behavior at the edge singularities (Fisher's edges). Probably the first hint of such similarity has appeared in [8] in the $d = 1$ Q-state Potts model where a duality between magnetic field and temperature has allowed one to prove that the singular behavior of the linear density ($\sigma = -1/2$) at Yang–Lee edge singularities (YLES) is carried forward to the Fisher edges. The Q-state Potts model in $d = 2$ (square lattice) and $d = 3$ (cubic lattice) has been investigated in [16] and led the author to conjecture that $y_T = y_H$ in $d = 1, 2, 3$. It has been argued in [19] that the existence of only one relevant scaling field in the $(p, q) = (2, 5)$ minimal model is behind the identity $y_T = y_H$ in the $d = 2$ spin-1/2 Ising model. Later, for the $d = 1$ Blume–Capel model, the authors of [9] have also shown that the divergence at Fisher edges is also of square-root type, $\sigma = -1/2$.

In this work we study, for real magnetic fields, all partition function zeros associated with the three different couplings (J, K, Δ) appearing, see (1), in the $d = 1$ spin-1 BEG model. This model includes the Blume–Capel model and the spin-1 and spin-1/2 Ising models. We show, in general, that the linear density of zeros diverges at the edge singularities (ES) like a square root ($\sigma = -1/2$) for all types of partition function zeros. The universality of the square-root divergence at edge singularities can be violated in the regions of the parameter space where the three transfer matrix eigenvalues become degenerate. In this case, a new critical behavior with $\sigma = -2/3$ can appear just like the case of complex magnetic field and real (J, K, Δ) investigated in [10, 22] and the case of the three-state Potts model in the presence of a magnetic field with two complex components studied earlier[1] in [23]. We confirm this new critical behavior with analytic and numerical results with the help of FSS relations. Different from the cases studied in [10], here the new critical behavior appears at the closest edges to the positive real axis which points out its possible physical relevance in higher-dimensional spin models with tricritical behavior.

2. The BEG model and the basic setup

One can interpret the BEG [24] model as a generalization of the spin-1 Ising model where two extra couplings Δ and K are introduced. They are associated with a quadrupole moment $\langle S_i^2 \rangle$, as in [25], and a quartic spin interaction $\langle S_i^2 S_j^2 \rangle$ among nearest neighbors, respectively. Explicitly we have

$$Z_N = \sum_{\{S_i\}} \exp\beta\left\{J\sum_{\langle ij\rangle} S_i S_j + K\sum_{\langle ij\rangle} S_i^2 S_j^2 + \sum_{i=1}^{N}\left[H S_i + \Delta\left(1 - S_i^2\right)\right]\right\}. \quad (1)$$

On each of the N sites we can have three possible spin states $S_i = 0, \pm 1$. The sums $\sum_{\langle ij\rangle}$ run over nearest-neighbor links. It is convenient to define the following quantities:

$$u = e^{\beta H}, \qquad c = e^{-\beta J}, \qquad b = e^{\beta K}, \qquad x = e^{\beta\Delta} \quad (2)$$

$$\tilde{x} = xc = e^{\beta(\Delta - J)}, \qquad A = u + \frac{1}{u} = 2\cosh(\beta H). \quad (3)$$

At $b = 1$ we recover the Blume–Capel model [25] while the spin-1 and spin-1/2 Ising models are obtained at $b = 1 = x$ and $x \to 0$, respectively.

In the one-dimensional case with periodic boundary conditions (one ring), it is easy to check that $Z_N(u, c, b, x)$ is proportional to a polynomial of degree $2N$ as a function of u (or c) but of degree N as a function of b (or x). For real couplings H, J, K, Δ, the partition function is a sum of non-negative terms and never vanishes. We must allow, at least, one of the couplings to become complex in order to have zeros. In [10] we have assumed a complex magnetic field, keeping J, K, Δ real numbers, and studied the so-called Yang–Lee zeros on the complex u-plane. Here, in contrast, we keep H real ($A \geqslant 2$) and suppose that one out of the three couplings J, K, Δ is complex with the two remaining ones being real. If the Ising coupling J is the complex one, the zeros on the complex c-plane will be called Fisher zeros (or c-zeros) in analogy with the denomination of complex-temperature zeros of the Ising model. Otherwise, we may take either K or Δ complex. The corresponding zeros will be called b-zeros and x-zeros, respectively. In the latter cases, the range of temperature $0 \leqslant T < \infty$ is mapped into the compact interval $0 \leqslant c \leqslant 1$ since $J > 0$.

[1] We thank the referee of *J. Phys. A* for bringing this reference to our knowledge.

Using periodic boundary conditions $S_i = S_{i+N}$ one easily obtains Z_N in terms of the transfer matrix eigenvalues λ_a/c $(a = 1, 2, 3)$:

$$Z_N = \mathrm{Tr}T^N = c^{-N}\left[\lambda_1^N + \lambda_2^N + \lambda_3^N\right]. \tag{4}$$

The quantities λ_a are the solutions of the cubic equation:

$$\lambda^3 - a_2\lambda^2 + a_1\lambda - a_0 = 0, \tag{5}$$

with

$$a_0 = bxc(1 - c^2)[b(1 + c^2) - 2c] \tag{6}$$

$$a_1 = b^2(1 - c^4) + Axc(b - c) \tag{7}$$

$$a_2 = xc + Ab. \tag{8}$$

At this point one might try to replace the explicit solutions of (5) in (4) and find the partition function zeros $z_i(N)$ for finite N. The variable z represents among the three quantities (b, c, x) the one which is assumed to be complex. It turns out that this procedure is not useful for large N. Thus, we follow a different route.

From (4) it is clear that as we approach the limit $N \to \infty$ we may have zeros of the partition function in two situations. Namely, either the three eigenvalues share the same absolute value $(|\lambda_1| = |\lambda_2| = |\lambda_3|)$ or two of them have the same absolute value which must be larger than the third one: $|\lambda_1| = |\lambda_2| > |\lambda_3|$. The first case, though not impossible (see subsection 3.2 of [22]), is very unlikely. We concentrate henceforth on the second possibility. In this case it is a good approximation at large N to disregard the third eigenvalue and write down $Z_N \approx \lambda_1^N(1 + \mathrm{e}^{\mathrm{i}N\varphi})$ where we have used the condition $\lambda_2 = \mathrm{e}^{\mathrm{i}\varphi}\lambda_1$. Therefore, the partition function zeros are given by $\varphi_k = (2k - 1)\frac{\pi}{N}, k = 1, 2, \ldots, N$. Since the edge singularity (ES), like any other second-order phase transition point [26, 27], corresponds to the double degeneracy of the largest eigenvalue $(\varphi = 0)$, it is expected that the smallest phase $\varphi_1 = \pi/N$ corresponds to the closest zero to the ES. So, following [9] and [10], we assume that one of the parameters (c, b, x) is complex and depends on the phase φ, i.e. $z = z(\varphi)$. It is such that after putting it back in (5) we obtain $\lambda_2 = \mathrm{e}^{\mathrm{i}\varphi}\lambda_1$. If the condition $|\lambda_1| = |\lambda_2| > |\lambda_3|$ is verified (this must be checked afterward), the following Taylor expansion becomes a good approximation at large N for the closest zero z_1 to the ES $z(0)$:

$$\begin{aligned} z_1 = z(\varphi)|_{\varphi=\pi/N} &= \left[z(0) + \varphi\left.\frac{\mathrm{d}z}{\mathrm{d}\varphi}\right|_{\varphi=0} + \frac{\varphi^2}{2!}\left.\frac{\mathrm{d}^2z}{\mathrm{d}\varphi^2}\right|_{\varphi=0} + \cdots\right]_{\varphi=\pi/N} \\ &= z(0) + \frac{\pi}{N}\left.\frac{\mathrm{d}z}{\mathrm{d}\varphi}\right|_{\varphi=0} + \frac{\pi^2}{2N^2}\left.\frac{\mathrm{d}^2z}{\mathrm{d}\varphi^2}\right|_{\varphi=0} + \cdots. \end{aligned} \tag{9}$$

On the other hand, for complex magnetic fields (Yang–Lee zeros or complex temperatures (Fisher zeros), it is known [11] that the closest zero to the phase transition point (ES) obeys the finite-size scaling (FSS) relation

$$z_1(L) = z_1(\infty) + \frac{C_1}{L^{y_z}} + \cdots, \tag{10}$$

where C_1 is a constant independent on the number of spins N and $L = N^d = N$. Comparing (9) and (10) it is clear that if we know the first derivatives $\mathrm{d}^nz/\mathrm{d}\varphi^n$ at $\varphi = 0$ we can determine the scaling exponent y_z analytically and consecutively the universal exponent $\sigma = (d - y_z)/y_z = (1 - y_z)/y_z$. It will be confirmed in this work that the FSS relation (10) holds also for b-zeros and x-zeros.

In principle, the function $z(\varphi)$ could be determined from the condition $\lambda_2 = e^{i\varphi}\lambda_1$ and the requirement $|\lambda_1| = |\lambda_2| > |\lambda_3|$ applied directly to the explicit solutions of the cubic equation (5). Unfortunately, except for the case of a vanishing magnetic field $H = 0$ (see the next section), the roots of (5) are so cumbersome that they are not really useful for determining $d^n z/d\varphi^n$ at $\varphi = 0$. Instead, as in [9, 10], we derive an implicit equation for $z(\varphi)$. Substituting the condition $\lambda_2 = e^{i\varphi}\lambda_1$ in the relations $a_0 = \lambda_1\lambda_2\lambda_3$, $a_1 = \lambda_1\lambda_2 + \lambda_1\lambda_2 + \lambda_2\lambda_3$, $a_2 = \lambda_1 + \lambda_2 + \lambda_3$, which are symmetric under permutations of the eigenvalues, we have

$$a_0 = \lambda_1^2\lambda_3\, e^{i\varphi}, \tag{11}$$

$$a_1 = \lambda_1\lambda_3 + e^{i\varphi}(\lambda_1^2 + \lambda_1\lambda_3), \tag{12}$$

$$a_2 = \lambda_3 + \lambda_1(1 + e^{i\varphi}). \tag{13}$$

Note that (11), (12) and (13) are invariant under

$$(\varphi, \lambda_1) \to (-\varphi, e^{i\varphi}\lambda_1), \tag{14}$$

which corresponds to the permutation $\lambda_1 \rightleftarrows \lambda_2$. If we eliminate λ_3 and λ_1 from the three equations (11), (12), (13), we end up with an implicit equation for $z(\varphi)$ which must be even under $\varphi \to -\varphi$ as a consequence of symmetry (14). Indeed from (11), (12) and (13) one derives

$$a_0^2\,(1 + 2\cos\varphi)^3 + 4\cos^2\frac{\varphi}{2}\left(a_1^3 + a_0a_2^3\right) - a_1^2a_2^2 - 2\,(1 + 2\cos\varphi)\,(2 + \cos\varphi)\,a_0a_1a_2 = 0. \tag{15}$$

Formula (15) has first appeared in [9] for the case of the Blume–Capel model ($b = 1$) and in [10] for the BEG model ($b \geqslant 0$). Expression (15) implicitly determines $z(\varphi)$ such that $\lambda_2 = e^{i\varphi}\lambda_1$. Condition (15) is a polynomial of degree (12, 6, 4) in (c, b, x), respectively. At $\varphi = 0$, equation (15) becomes the double degeneracy condition for the eigenvalues of the cubic equation (5). We remark that not all solutions of (15) satisfy the condition $|\lambda_2| = |\lambda_1| > |\lambda_3|$ which must be checked afterward.

Although (15) is even under $\varphi \to -\varphi$, its analytic solutions about $\varphi = 0$ do not need to be so. There could be an interchange among the multiple solutions of (15) under $\varphi \to -\varphi$. Consequently, the odd derivatives $d^{2n+1}z/d\varphi^{2n+1}$ at $\varphi = 0$ are not necessarily zero[2]. More explicitly, the first derivative of (15) at $\varphi = 0$, with the help of (11), (12) and (13), can be written as

$$(\lambda_1 - \lambda_3)^3|_{\varphi=0}\left[-\lambda_1^2\frac{da_2}{d\varphi} + \lambda_1\frac{da_1}{d\varphi} - \frac{da_0}{d\varphi}\right]_{\varphi=0} = 0. \tag{16}$$

Therefore, if there is no triple degeneracy ($\lambda_1 = \lambda_2 \neq \lambda_3$) at the edge singularity ($\varphi = 0$), the term inside the brackets in (16) must vanish and since $da_i/d\varphi \propto dz/d\varphi$ we expect, except at very special points in the parameters space of the model, $(dz/d\varphi)_{\varphi=0} = 0$. Proceeding further, using $(dz/d\varphi)_{\varphi=0} = 0$, the second and third derivatives of (15) at $\varphi = 0$ become

$$(\lambda_1 - \lambda_3)^3|_{\varphi=0}\left[-\lambda_1^2\frac{d^2a_2}{d\varphi^2} + \lambda_1\frac{d^2a_1}{d\varphi^2} - \frac{d^2a_0}{d\varphi^2} + \frac{\lambda_1\,(\lambda_1 - \lambda_3)}{2}\right]_{\varphi=0} = 0, \tag{17}$$

[2] The skeptical reader can look at the simpler equation $z^2 + 2z\cos\varphi + 1 = 0$. One might think that due to the symmetry $\varphi \to -\varphi$, each solution must be separately even: $z_\pm(-\varphi) = z_\pm(\varphi)$, and consequently they will have only even powers of φ when expanded about $\varphi = 0$. However, the above equation is everywhere equivalent to $(z - e^{i\varphi})(z - e^{-i\varphi}) = 0$ whose analytic solutions $z_\pm(\varphi) = e^{\pm i\varphi}$ have no definite parity. Their expansions about $\varphi = 0$ contain even and odd powers of φ. The symmetry $\varphi \to -\varphi$ simply interchanges the solutions $z_+ \leftrightarrow z_-$.

$$(\lambda_1 - \lambda_3)^3|_{\varphi=0}\left[-\lambda_1^2\frac{d^3a_2}{d\varphi^3} + \lambda_1\frac{d^3a_1}{d\varphi^3} - \frac{d^3a_0}{d\varphi^3}\right]_{\varphi=0} = 0. \tag{18}$$

In summary, except at the triple degeneracy point $\lambda_1 = \lambda_2 = \lambda_3$ and at very special points in the parameter space of the BEG model, we have $(dz/d\varphi)_{\varphi=0} = 0 = (d^3z/d\varphi^3)_{\varphi=0}$ while $(d^2z/d\varphi^2)_{\varphi=0} \neq 0$ which implies, see (9) and (10), that $y_z = 2$ and $\sigma = -1/2$. This is the well-known result for the critical exponent σ in one-dimensional spin models with short-range interactions and complex magnetic fields [3, 8, 12, 13]. It seems to hold also at complex temperatures [9]. We have just shown, generalizing [9], that the same exponent $\sigma = -1/2$ appears for more general partition function zeros associated with other complex couplings in the model as far as we do not have a triple degeneracy of the transfer matrix eigenvalues. Equations (16), (17) and (18), derived from (15), follow from the fact that $\frac{d^n\cos(\varphi)}{d\varphi^n}\Big|_{\varphi=0}$ does (not) vanish for odd (even) 'n' which, on its turn, is a consequence of the invariance of (11), (12) and (13) against (14) which represents the permutation $\lambda_1 \leftrightarrows \lambda_2$. So, we have a general proof of universality of $\sigma = -1/2$ for arbitrary partition function zeros for three-state spin models which we believe could be generalized for multiple-state spin models. In particular, the specific details regarding the functions $a_i\,(H, \Delta, K, J)$, $i = 0, 1, 2$, given in (6), (7) and (8) play no important role in proving $\sigma = -1/2$.

For complex magnetic fields we have already shown in [10, 22] that, though not sufficient, the condition $\lambda_1 = \lambda_2 = \lambda_3$ may indeed lead to a new critical behavior at the ES with $\sigma = -2/3$ ($y_H = 3$). In the rest of this work we search for the triple degeneracy case at the real magnetic field ($A \geqslant 2$).

Our conclusions are confirmed by high-precision numerical computations of the partition function zeros. In the numerical approach, the roots of the polynomials are found with the help of the software Mathematica. The polynomials are generated by an alternative [10, 22] expression for the partition function

$$Z_N = -\frac{1}{c^N(N-1)!}\left[\frac{d^N}{dg^N}\ln(1 - a_2g + a_1g^2 - a_0g^3)\right]_{g=0}. \tag{19}$$

As explained in [22, 28], expression (19) is obtained from a diagrammatic interpretation of the (one-ring) partition function for N spins in terms of Feynman diagrams with N vertices of two-lines (zero-dimensional Gaussian field theory). The constant 'g' is a coupling constant in the corresponding field theory. Expression (19) turns out to be computationally much more efficient than $\mathrm{tr}\,T^N$. After obtaining the exact zeros (with high accuracy) we compare two rings of different number of spins N_a and N_{a+1} and derive, using the FSS relation (10), y_z from

$$y_z = -\left[\ln\frac{N_{a+1}}{N_a}\right]^{-1}\ln\left[\frac{\Delta z_1(N_{a+1})}{\Delta z_1(N_a)}\right]. \tag{20}$$

Both the imaginary and real part of the zeros, i.e. $\Delta z_1(N) = \mathrm{Im}[z_1(N) - z_1(N\to\infty)]$ and $\Delta z_1(N) = \mathrm{Re}[z_1(N) - z_1(N\to\infty)]$ can be used in (20). The value[3] of $z_1(N\to\infty)$ is obtained from (15) at $\varphi = 0$.

Moreover, we also numerically calculate the density of zeros about the edge singularity using the first two closest zeros to the edge ending point:

$$\rho(N) = \frac{1}{N|z_1(N) - z_2(N)|}, \tag{21}$$

and from another FSS relation, see [11, 29],

$$\rho(N) = C_2L^{y_z-d} = C_2N^{y_z-1}, \tag{22}$$

[3] Approximate values of $z_1(N\to\infty)$ can be found from a three-parameter nonlinear fit of (10) without the use of (15). We have done so as a double check.

we have, similar to (20),

$$y_z = 1 + \left[\ln \frac{N_{a+1}}{N_a}\right]^{-1} \ln\left[\frac{\rho(N_{a+1})}{\rho(N_a)}\right]. \tag{23}$$

In the next section we first analyze the simplest case of a vanishing magnetic field.

3. Vanishing magnetic field: $(A = 2)$

We illustrate the landscape of x-zeros, b-zeros and c-zeros at $H = 0$ in figure 1(a), (b) and (c), respectively. The case of a vanishing magnetic field ($A = 2$) is special since the cubic equation (5) factorizes, leading to simple formulae for the eigenvalues:

$$\lambda_\pm = \tfrac{1}{2}[R \pm \sqrt{S}], \tag{24}$$

$$\lambda_3 = b(1 - c^2), \tag{25}$$

with $R = x\,c + b(1 + c^2)$ and $S = [x\,c + b(1 + c^2)]^2 + 8x\,c^2$. As explained in the last section, a new critical behavior at the edge singularity can only appear at the triple degeneracy point $\lambda_+ = \lambda_- = \lambda_3$, which implies

$$xc = b(1 - 3c^2), \tag{26}$$

$$2bc^3 = -(1 - 3c^2). \tag{27}$$

On the other hand, from the condition $\lambda_+ = \mathrm{e}^{\mathrm{i}\varphi}\lambda_-$ we obtain the equation

$$[xc - b(1 + c^2)]^2 + 4xc^2(1 + \cos\varphi) + 2xbc(1 + c^2)(1 - \cos\varphi) = 0. \tag{28}$$

Equation (28) at $\varphi = 0$ will be automatically satisfied due to (26) and (27). By taking derivatives of (28) at $\varphi = 0$ we collect information about $\mathrm{d}^n z/\mathrm{d}\varphi$ at $\varphi = 0$. For definiteness let us look first at x-zeros, i.e. $z(\varphi) = x(\varphi)$. The edge is located, by virtue of (26) and (27), on the negative real axis on the complex x-plane: $x_E = -(1 - 3c^2)^2/(2c^4)$. We must assume that $1/\sqrt{3} < c < 1$ since $b = (3c^2 - 1)/(2c^3)$ should be positive ($K \epsilon \mathbb{R}$). Numerical computations of the zeros confirm our analytic analysis.

From the first derivative of (28) at $\varphi = 0$, we have $(1 - bc)\frac{\mathrm{d}x}{\mathrm{d}\varphi}\big|_{\varphi=0} = 0$. Due to (26) and (27) we can only have $bc = 1$ if $c = \pm 1$, but since $1/\sqrt{3} < c < 1$ we conclude that

$$\left.\frac{\mathrm{d}x}{\mathrm{d}\varphi}\right|_{\varphi=0} = 0. \tag{29}$$

By using this fact and the triple degeneracy conditions (26) and (27), we deduce from the second derivative of (28) at $\varphi = 0$:

$$\left.\frac{\mathrm{d}^2x}{\mathrm{d}\varphi^2}\right|_{\varphi=0} = \frac{1 - c^2}{4c}. \tag{30}$$

Since $\frac{\mathrm{d}^2x}{\mathrm{d}\varphi^2}\big|_{\varphi=0} \neq 0$, from the Taylor expansion (9) and the FSS relation (10) we find $y_\Delta = 2$ which implies the usual critical exponent $\sigma = -1/2$. The alternative condition $\lambda_+ = \mathrm{e}^{\mathrm{i}\varphi}\lambda_3$ also leads to $\sigma = -1/2$. Therefore, we can only have x-zeros with a new critical behavior $\sigma \neq -1/2$ for a non-vanishing magnetic field ($A > 2$) which will be investigated in section 4.

Now we examine the case of the b-zeros at $H = 0$ ($A = 2$), i.e. complex K but real Δ and $J > 0$ ($0 \leqslant c \leqslant 1$). It is clear from (26) that b_E must be a real number. Consequently, we must have the coupling K purely imaginary which implies $b_E < 0$ and requires $0 < c < 1/\sqrt{3}$.

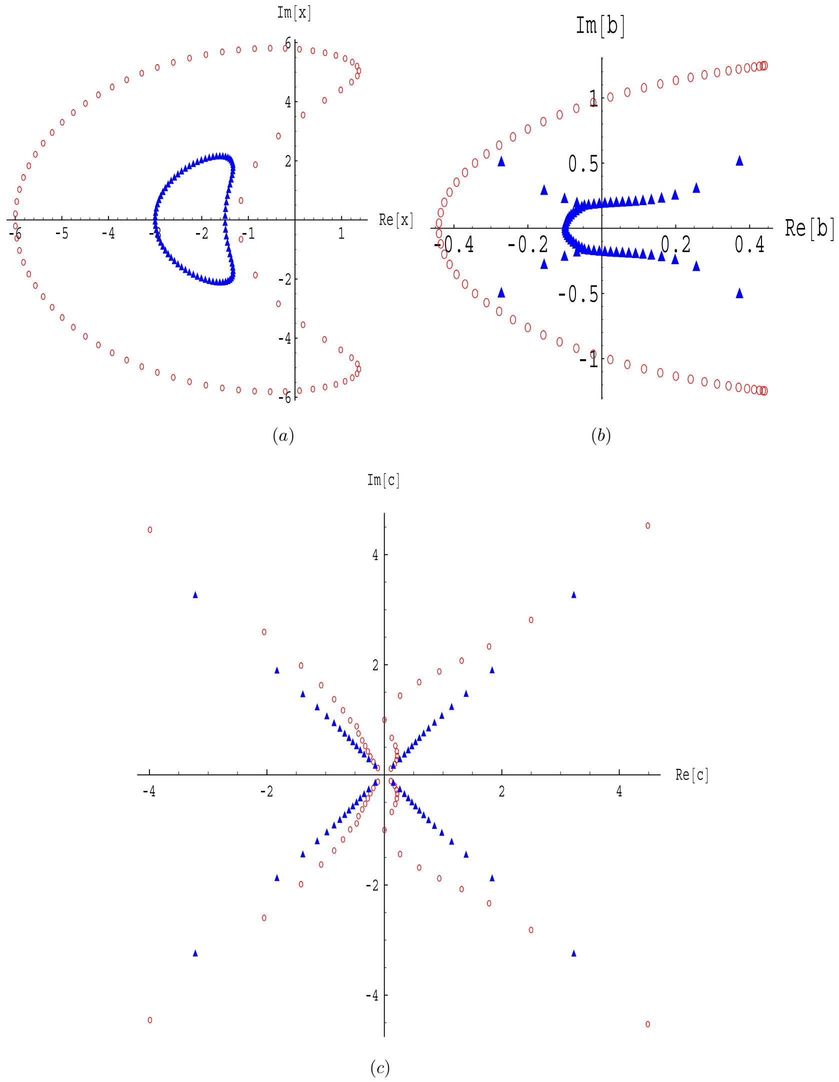

Figure 1. x-zeros, b-zeros and c-zeros at $H = 0\,(A = 2)$: (a) x-zeros with $(b, A) = (1, 2)$ for $n = 80$ spins at $c = 0.5$ (blue triangles) and $c = 0.2$ (red circles); (b) b-zeros with $(x, A) = (1, 2)$ for $n = 60$ spins at $c = 0.1$ (blue triangles) and $c = 0.6$ (red circles); (c) c-zeros with $(b, A) = (1, 2)$ for $n = 60$ spins at $x = 0.1$ (blue triangles) and $x = 1.0$ (red circles).

However, in this case, (26) and (27) lead to $x = -2b_E^2c^2 < 0$ which is forbidden for real Δ. Therefore, there can only be b-zeros with a new critical behavior if $H \neq 0\,(A > 2)$. There is no need of investigating the derivatives $\mathrm{d}^n b/\mathrm{d}\varphi$ at $\varphi = 0$. The situation is similar for the c-zeros, i.e. complex J, real Δ ($x \geqslant 0$) and real K ($b \geqslant 0$). Since the triple degeneracy conditions imply $x = -2b^2c_E^2$ we must have c_E purely imaginary but then (27) requires complex b. So we conclude that there are no partition function zeros with a new critical behavior ($\sigma \neq -1/2$) at the vanishing magnetic field. In the next sections we search for a new critical behavior assuming $H \neq 0$.

4. Non-vanishing magnetic field ($A > 2$)

4.1. x-zeros

4.1.1. $b \geqslant 1$. The solutions of the cubic equation (5) coalesce at $\lambda_1 = \lambda_2 = \lambda_3 = a_2/3$ if and only if $3\,a_1 - a_2^2 = 0$ and $a_1\,a_2 - 9\,a_0 = 0$, which implies respectively

$$x^2c^2 + b^2A^2 + A(xc)(3c - b) = 3b^2(1 - c^4), \tag{31}$$

$$x^2c^2A(b - c) + A^2(xc)b(b - c) + Ab^3(1 - c^4) = xcb(1 - c^2)[8b(1 + c^2) - 18c]. \tag{32}$$

In [10] we were interested in Yang–Lee zeros which appear for the complex magnetic field and real couplings (Δ, K, J). For the special values $b = 1$ (Blume–Capel model) and $b = c$ $(K = -J)$ we have been able to solve in [10] the couple of algebraic equations (31) and (32) in terms of specific functions of the temperature $x(c)$ and $A_E(c)$. The function $A_E(c)$ gives the position of the YLES for each temperature while $x(c)$, which satisfies $x(c) \geqslant 0$ for the whole range of real temperatures $(0 \leqslant c < 1)$, guarantees the triple degeneracy condition of the transfer matrix eigenvalues at the edge, see [10]. Now the situation is more involved. For example, for x-zeros (complex Δ) all the constraints $b \geqslant 0$, $0 \leqslant c \leqslant 1$ and $A > 2$ must be fulfilled. By combining (31) and (32) we can find the position of the YLES on the complex x-plane, assuming that the denominator below is non-vanishing:

$$x_E(A, b, c) = \frac{Ab^2[A^2(b - c) - (4b - 3c)(1 - c^4)]}{c[A^2(b - c)(2b - 3c) + 18bc(1 - c^2) - 8b^2(1 - c^4)]}. \tag{33}$$

By substituting $x_E(A, b, c)$ above in (31) we have in general an algebraic cubic equation for A^2 as the function of b and c. Two of the solutions are in general complex. A three-dimensional plot of the third (real) solution in the two-dimensional compact region $0 \leqslant (1/b) \leqslant 1$ with $0 \leqslant c \leqslant 1$ reveals that $0 \leqslant A < 2$. Recalling that $A > 2$, we conclude that, as far as the denominator of (33) is non-vanishing, there are no x-zeros with a new critical behavior at the ES in the BEG model with $b \geqslant 1$ $(K \geqslant 0)$.

On the other hand, back to (33), imposing the vanishing of the denominator (and numerator), we obtain two temperature-dependent conditions for the magnetic field H and the coupling K, respectively:

$$A = \sqrt{4 + 2c^2(1 - c^2)}, \tag{34}$$

$$b = \frac{1 + c^2}{2c}. \tag{35}$$

It is an acceptable solution satisfying $2 < A \leqslant 3\sqrt{2}/2$ (or approximately $0 < H/k_BT \leqslant 0.35$) and $b > 1$. It does not include the Blume–Capel model $(b = 1)$. Replacing (34) and (35) in (31) we obtain the location of the edge singularities on the complex x-plane:

$$x_E^{\pm} = \frac{1}{2c^2}\sqrt{\frac{1 + c^2}{2}}[(1 - 5c^2)\sqrt{2 - c^2} \pm 3c(1 - c^2)\sqrt{3}\mathrm{i}]. \tag{36}$$

Conditions (34), (35) and (36) guarantee for any finite temperature that there is a pair of real couplings (K, H) which leads to a couple of complex values of $x = \mathrm{e}^{\beta\Delta}$ such that $\lambda_1 = \lambda_2 = \lambda_3$. In order to confirm that $x_E^{\pm}$ correspond to true edge singularities and calculate σ, we have to study the vicinity of $x_E^{\pm}$. Substituting (34) and (35) in the condition $\lambda_2 = \mathrm{e}^{\mathrm{i}\varphi}\lambda_1$, equation (15), we obtain a fourth-degree polynomial for $x(\varphi)$ which can be solved perturbatively about $\varphi = 0$. The first solution can be written as

$$x_I(\varphi) = x_E^+ + c_3(c)\varphi^3 + c_4(c)\varphi^4 + \cdots, \tag{37}$$

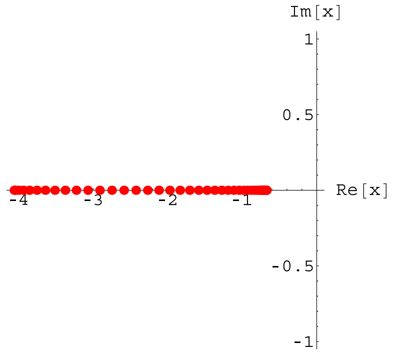

Figure 2. x-zeros for $n = 40$ spins with $A \approx 2.0045$ and $b = c = 0.8$.

where $c_3(c), c_4(c), \ldots$ are complicated temperature-dependent coefficients. We have checked that c_3 and c_4 never vanish. The second perturbative solution of φ corresponds to $x_{II}(\varphi) = x_I^*(\varphi)$. Putting back these couple of solutions in (5) together with (34) and (35) we can obtain the three eigenvalues $\lambda_a(\varphi)$, $a = 1, 2, 3$, perturbatively in the vicinity of $\varphi = 0$. A plot of $|\lambda_i(\varphi)|$ reveals that $\lambda_1 = \lambda_2 = \lambda_3$ at $\varphi = 0$ and $|\lambda_1(\varphi)| = |\lambda_2(\varphi)| > |\lambda_3(\varphi)|$ about $\varphi = 0$. Therefore we confirm that x_E^+ and $x_E^- = \left(x_E^+\right)^*$ are true edge singularities. Comparing (37) with (20) we find $y_\Delta = 3$ and $\sigma = -2/3$. The remaining two perturbative solutions of (15) with conditions (34) and (35) are $x_{III}(\varphi) = x_I(-\varphi)$ and $x_{IV}(\varphi) = x_{II}(-\varphi)$, which are in agreement with the $\varphi \to -\varphi$ symmetry of (15). It can be checked that they imply $|\lambda_1(\varphi)| = |\lambda_2(\varphi)| < |\lambda_3(\varphi)|$ and consequently $x_{III}(\varphi)$ and $x_{IV}(\varphi)$ do not describe the neighborhood of the edge singularities $x_E^\pm$ along a curve of partition zeros and must be disregarded.

The above results have been crosschecked by numerical computations of x-zeros. First of all we have verified by means of di-log fits that the FSS relations (10) and (22) hold also for x-zeros, see for instance figure 3(b) and 3(a) where we have assumed $c = 0.1$ and $x_1(N \to \infty) = x_E^+$ given in (36). From the di-log fits, shown in figure 3(a) and 3(b), respectively, we have a rough estimate $y_\Delta^E = 2.92$ or $y_\Delta^{(\rho)} = 2.86$. The quality of the fits have been measured by $\chi_E^2 = 2.4 \times 10^{-6}$ and $\chi_\rho^2 = 1.1 \times 10^{-5}$ and for obtaining y_Δ^E from (10) we have used the real part of the zeros. The use of the imaginary part would lead to a worse result $\left(y_\Delta^E = 3.20\right)$ as expected from the position of the zeros close to the ES, see figure 5(a) and (b).

Now assuming that (10) and (22) are correct, we can have a better estimate of y_Δ from (20) and (23), see the example in table 1 at the temperature $c = 0.5$ with $A \approx 2.091\,65$ and $b = 1.25$ obtained from (34) and (35), respectively. In the last row we have used the BST (Burlish–Stör) extrapolation algorithm, see [30, 31], which approximates the sequence $y_\Delta(N_a)$ by another sequence of ratios of polynomials with faster convergence. The BST approach depends upon one real parameter ω which appears in the expansion $y_\Delta(N) = y_\Delta(\infty) + \frac{A_1}{N^\omega} + \frac{A_2}{N^{2\omega}} + \cdots$. We have chosen $\omega = 1$ in table 1, as in [10]. In figure 4(a), (b) and (c), obtained at the temperature $c = 0.1$, we plot the extrapolated quantity $y_\Delta(\infty)$ for $0.2 \leqslant \omega \leqslant 3.0$ altogether with their error bars which are defined, following [30], as twice the difference between the two approximants for $y_\Delta(\infty)$ generated in the step before the last iteration of the BST algorithm. Note the smaller deviation about $y_\Delta = 3.0$ in figure 4(b) compared to 4(c) which can be explained by the fact that, see figure 5, the zeros at $c = 0.1$ approach the ES more horizontally than vertically. The relative difference in the real part of the zeros is much larger than that in

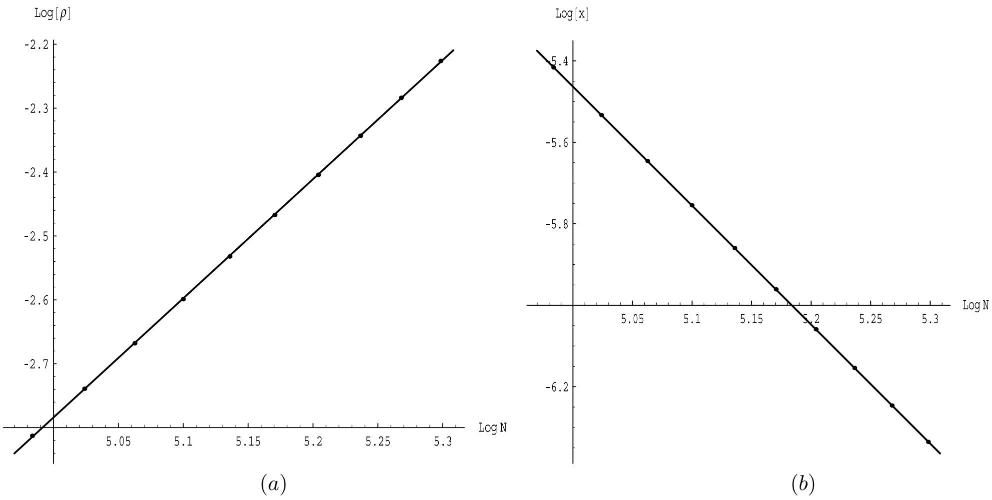

Figure 3. Di-log fits for x-zeros with $c = 0.1$, $A = \sqrt{4 + 2c^2 - 2c^4} \approx 2.004\,94$, $b = (1+c^2)/2c = 5.05$ and $146 \leqslant N \leqslant 200$ spins. (a) Di-log fit of (22): $\log\rho = -12.109 + 1.865\ \log N$, ($b$) Di-log fit of (10): $\log\ \Delta x = 9.144 - 2.921\ \log N$.

Table 1. Finite-size results for the x-zeros, where y_Δ^ρ are obtained from (21) while $y_\Delta^{E,\,\mathrm{Re}}$ and $y_\Delta^{E,\,\mathrm{Im}}$ come from (20) using the real and imaginary parts of the zeros, respectively. The zeros have been calculated for $146 \leqslant N \leqslant 194$ spins at $c = 0.5$, $A \approx 2.091\,65$ and $b = 1.25$. The last row is the $N \to \infty$ extrapolation via the BST algorithm with $\omega = 1$

N_a	y_Δ^ρ	$y_\Delta^{E,\,\mathrm{Re}}$	$y_\Delta^{E,\,\mathrm{Im}}$
146	2.996 000 201 99	3.101 330 448 91	2.995 888 796 78
152	3.003 943 031 45	3.015 493 490 28	3.000 788 750 52
158	3.001 424 208 92	2.999 753 577 81	3.000 131 175 92
164	2.999 988 158 42	3.000 009 312 33	3.000 000 027 96
170	3.000 000 005 00	3.000 000 823 39	2.999 999 999 22
176	3.000 000 005 98	3.000 000 003 15	2.999 999 999 80
182	3.000 000 005 17	3.000 000 001 06	3.000 000 000 05
188	2.999 999 999 99	2.999 999 999 28	3.000 000 000 00
∞	3.000 000 000 00(8)	3.000 000 000 00(9)	3.000 000 000 00(3)

the imaginary one as we get close to the ES. Thus, it is expected that the imaginary part of the zeros gives a worse estimate of y_Δ than the real one in this case, contrary to the case $c = 0.5$ where the situation is the opposite, see figures 6(b), (c) and 7.

4.1.2. The case $b = c$. The region $0 \leqslant b < 1$ is rather complicated but in the special case $b = c$ ($K = -J$) the edge position (33) becomes

$$x_E = -\frac{c(1+c^2)A}{2(5-4c^2)}, \tag{38}$$

where

$$A = \frac{2(5-4c^2)}{3}\sqrt{\frac{1+c^2}{3(1-c^2)}} \equiv A(c) \tag{39}$$

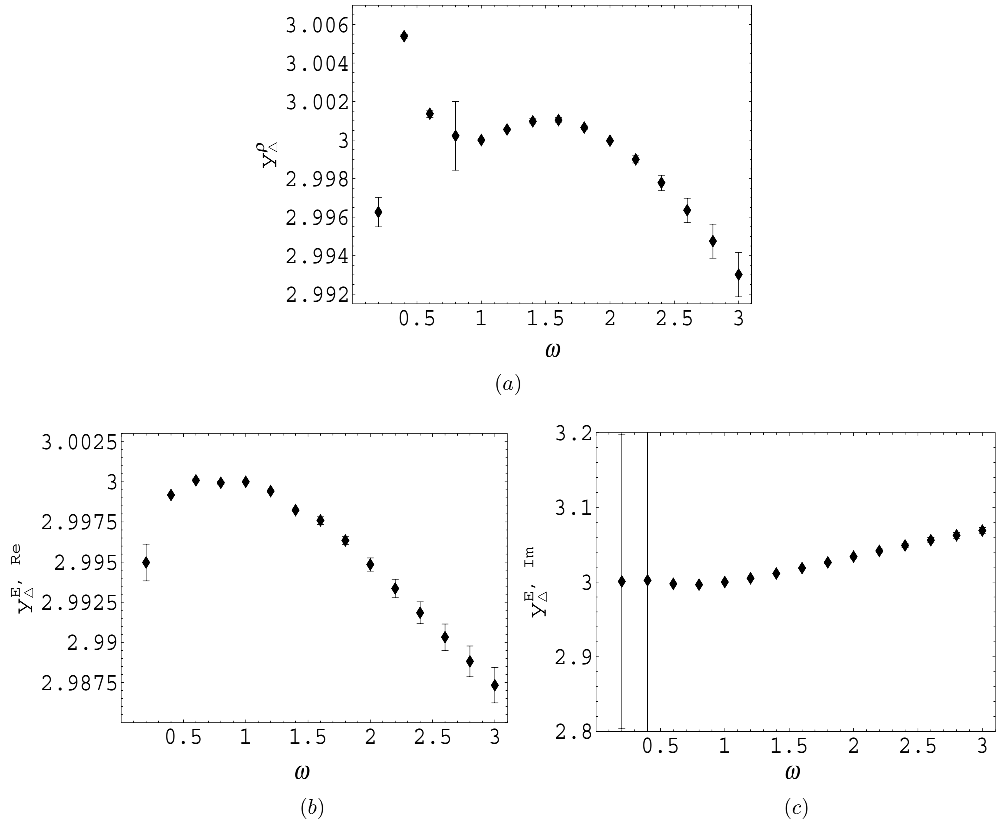

Figure 4. BST extrapolation for $0.2 \leqslant \omega \leqslant 3.0$ of y_Δ^ρ (a), and y_Δ^E (b) and (c), using the real and imaginary parts of the zeros, respectively. The x-zeros are calculated at $c = 0.1$, $A = 2.004\,94$ and $b = 5.05$.

is obtained by plugging back (38) in the triple degeneracy condition (31). For temperatures $\sqrt{2}/2 < c < 1$ we have $A(c) > 2$ as required and $x_E < 0$ (pure imaginary coupling Δ). Now we need to study the neighborhood of (38) in order to find y_Δ. After using (39), equation (15) becomes at $b = c$ a cubic equation for $x(\varphi)$ at each given temperature. As an example we choose the temperature $c = 0.8$. The first solution, see below, is an even function $x_I(-\varphi) = x_I(\varphi)$ while the other two have no definite parity:

$$x_I(\varphi) = -\frac{142\sqrt{123} + 61\sqrt{366}}{675} + \frac{9}{200}\sqrt{\frac{183}{2}}\varphi^2 + \mathcal{O}(\varphi^4), \tag{40}$$

$$x_{II}(\varphi) = -\frac{41}{225}\sqrt{\frac{41}{3}}\left(1 + \frac{3\sqrt{3}\varphi^3}{14} + \mathcal{O}(\varphi^4)\right), \tag{41}$$

$$x_{III}(\varphi) = x_{II}(-\varphi). \tag{42}$$

The quantity $x_{II}(\varphi = 0) = x_{III}(\varphi = 0)$ coincides with (38) at $c = 0.8$. Substituting $x_{II}(\varphi)$ in the cubic equation (5), we obtain perturbative expressions for the eigenvalues of the transfer matrix about $\varphi = 0$ such that $\lambda_1 = \lambda_2 = \lambda_3$ at $\varphi = 0$ and $|\lambda_1(\varphi)| = |\lambda_2(\varphi)| > |\lambda_3(\varphi)|$ about $\varphi = 0$. This confirms that x_E given in (38) is a true edge singularity. The Taylor expansion

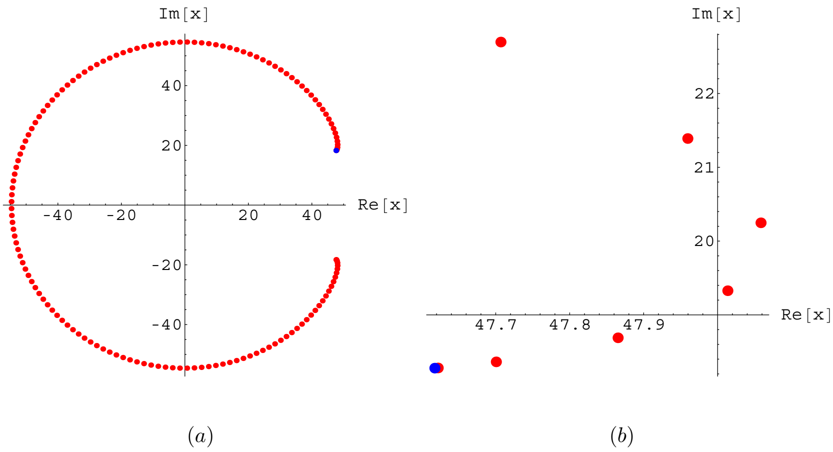

Figure 5. (*a*) x-zeros for $N = 146$ spins at $c = 0.1$, $A = \sqrt{4 + 2c^2 - 2c^4} \approx 2.0049$ and $b = (1 + c^2)/2c = 5.05$. (*b*) The seven closest zeros to the upper edge $x_E^+ \approx 47.6174 + 18.2781\,i$ obtained from (36). The blue/eighth dot (farthest to the left) stand for x_E^+.

(41) leads to $y_\Delta = 3$ and $\sigma = -2/3$ as we have argued before, see (9) and (10). Instead, if we use $x_{III}(\varphi)$ in (5) we get, besides $\lambda_1 = \lambda_2 = \lambda_3$ at $\varphi = 0$, $|\lambda_1(\varphi)| = |\lambda_2(\varphi)| < |\lambda_3(\varphi)|$ about $\varphi = 0$; therefore, $x_{III}(\varphi)$ does not describe the neighborhood of the edge singularity x_E along a curve of partition zeros and must be neglected. The case of $x_I(\varphi)$ leads to double degeneracy of the eigenvalues at $\varphi = 0$, i.e. $\lambda_1 = \lambda_2 \neq \lambda_3$ and $|\lambda_1(\varphi)| = |\lambda_2(\varphi)| > |\lambda_3(\varphi)|$. Thus, $x_I(\varphi)$ correctly describes the vicinity of a usual ($y_\Delta = 2, \sigma = -1/2$) ES. In summary, we have both types of edge singularities simultaneously, see figure 2, at $c = 0.8 = b$ and $A = A(c) \approx 2.0045$ (or $|H|/k_BT = 0.067$). Namely, only at the right edge ($x \approx -0.67$), we have $\lambda_1 = \lambda_2 = \lambda_3$ while at the left one ($x \approx -4.06$) we have verified that $\lambda_1 = \lambda_2 \neq \lambda_3$. Similar results appear for other temperatures in the range $\sqrt{2}/2 < c < 1$.

In conclusion, we have verified that the x-zeros do satisfy the FSS relations (10) and (22). Moreover, we have crosschecked that it is possible to have edge singularities with new critical behavior ($\sigma = -2/3$) for x-zeros (complex Δ) in both domains $b > 1$ and $b < 1$, similar to what we have obtained for Yang–Lee zeros (complex magnetic field) in [10]. As in [10], we need to fine tune the remaining (real) couplings (J, K, H) of the model in order to have triple degeneracy of the transfer matrix eigenvalues. Although this does not guarantee the new critical behavior, it is a necessary condition as we have analytically proved in (16), (17) and (18). Differently from [10], here we find no new critical behavior for x-zeros for the Blume–Capel model ($b = 1$).

4.2. b-zeros

It is not difficult to manipulate the triple degeneracy conditions (31) and (32) and isolate a function $b = b(A, c, x)$ as a ratio of two quite-involved functions $b = f_2(A, c, x)/f_1(A, c, x)$. Plugging this ratio back in (31), assuming of course that $f_1(A, c, x)$ never vanishes, we end up with a rather long expression $F(A, c, x) = 0$. We have made a 3D plot of $F(A, c, x)$ in the compact 2D domain: $0 \leqslant 1/A \leqslant 1/2$, $0 \leqslant c \leqslant 1$ for a list of values of the parameter x such that $0.01 \leqslant x \leqslant 4.01$; see, e.g., figure 8 obtained at $x = 2$. It turns out that $F(A, c, x) > 0$.

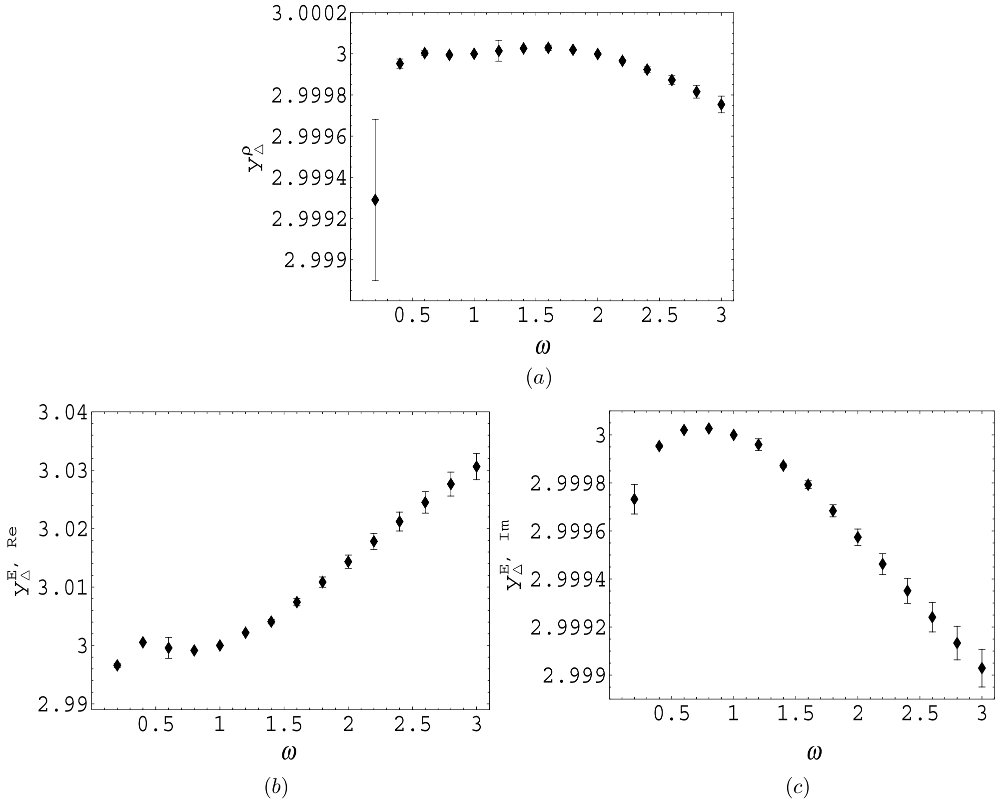

Figure 6. BST extrapolation for $0.2 \leqslant \omega \leqslant 3.0$ of y_{Δ}^{ρ} (a), and y_{Δ}^{E} (b) and (c), using the real and imaginary parts of the zeros, respectively. The x-zeros are calculated at $c = 0.5$, $A \approx 2.091\,65$ and $b = 1.25$.

Therefore, we believe that there are no b-zeros with new critical behavior ($\sigma = -2/3$) as far as $f_1(A, c, x) \neq 0$ (and $f_2(A, c, x) \neq 0$).

If $f_1(A, c, x) = 0$ we derive

$$x = -\frac{A[2A^2 - 9(1 - c^4)]^2}{[A^2 - 4(1 - c^4)][A^2 - 6(1 - c^4)]}, \tag{43}$$

where $A = \sqrt{V(1 - c^4)}$ is obtained by substituting expression (43) back in the numerator $f_2(A, c, x) = 0$. The quantity V satisfies the fourth-degree equation

$$V^4(1 + c^2) - V^3(15 + 13c^2) + 8V^2(10 + 7c^2) - 9V(9c^2 + 19) + 108 = 0. \tag{44}$$

Two of the solutions of (44) are complex numbers for finite temperatures ($0 \leqslant c < 1$) while another one is such that $A < 2$. Those three solutions lead to complex magnetic fields. However, there is always one real solution in the approximate range $2 < A < 2.13$ ($|H|/k_B T \leqslant 0.36$). Using such solution and substituting $A = \sqrt{V(1 - c^4)}$ altogether with x given in (43), in formula (15) we obtain a sixth-order polynomial for $b(\varphi)$. All solutions obtained in the neighborhood of $\varphi = 0$ appear in complex conjugated pairs as expected. In order to understand their meaning we introduce them back in (5) and obtain $\lambda_i(\varphi)$, $i = 1, 2, 3$, in the vicinity of $\varphi = 0$. For a couple of those solutions, say $b_1(\varphi), b_2(\varphi)$, where $b_2(\varphi) = b_1^*(\varphi)$, we have only a double degeneracy $\lambda_1 = \lambda_2 \neq \lambda_3$ at $\varphi = 0$ and they correspond to typical ES with $\sigma = -1/2$. The other four solutions are duplicated, i.e.

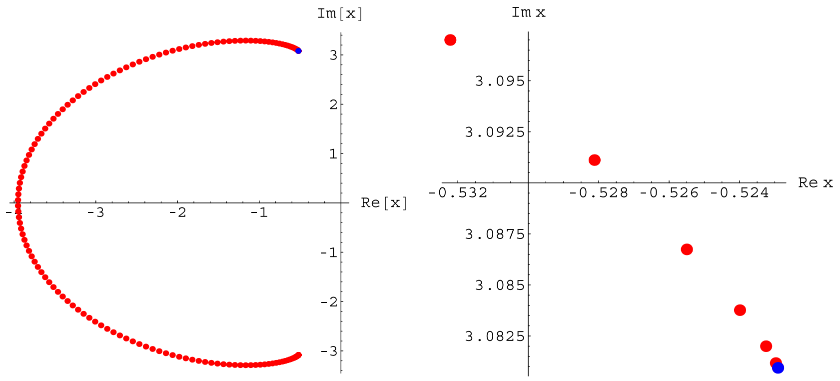

(*a*) (*b*)

Figure 7. (*a*) *x*-zeros for $N = 146$ spins at $c = 0.5$, $A = \sqrt{4+2c^2-2c^4} \approx 2.091\,65$ and $b = (1+c^2)/2c = 1.25$. (*b*) The seven closest zeros to the upper edge $x_E^+ \approx -0.522\,913+3.080\,94\,i$ obtained from (36). The blue dot/dot at the upper edge in (*a*) and at the bottom in (*b*) stand for x_E^+ and hide the almost coinciding zero x_1.

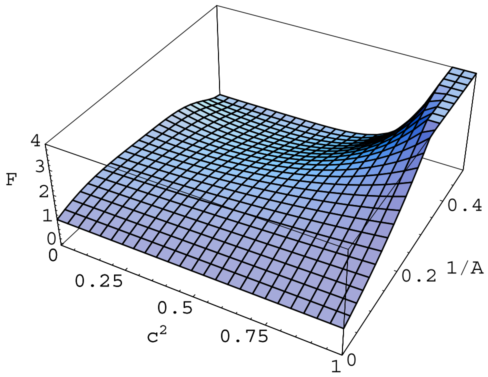

Figure 8. A 3D plot of $F(A, c, x)$ in the compact 2D domain: $0 \leqslant 1/A \leqslant 1/2$, $0 \leqslant c \leqslant 1$ for $x = 2$.

$b_3(\varphi) = b_5(\varphi)$ and $b_4(\varphi) = b_6(\varphi)$, with $b_4(\varphi) = b_3^*(\varphi)$. They both lead to triple degeneracy at $\varphi = 0$ and $|\lambda_1(\varphi)| = |\lambda_2(\varphi)| > |\lambda_3(\varphi)|$ in the vicinity of $\varphi = 0$, which means a true ES with $\sigma = -2/3$.

In conclusion, the situation is quite similar to the *x*-zeros in the case $b \geqslant 1$. Namely, there is a small window of real magnetic fields for which the ES shows up with a new critical behavior ($\sigma = -2/3$) also for *b*-zeros (complex *K*). The existence of this new behavior requires three conditions on the parameter space of the BEG model. Two of them, require the couple (A, x) to be specific functions of the temperature, see (43) and (44), and the third one fixes the position of the ES on the complex *b*-plane.

Our numerical results for *b*-zeros confirm $y_K = 3$ ($\sigma = -2/3$). Some of them are shown in figure 9(*a*) and (*b*) at $c = 0.5$. The results fit the FSS relations (10) and (22) once again. The *b*-zeros in figure 9(*a*) and (*b*) reinforce the choice $\omega = 1$ for the BST method. This is also a good choice of ω for the case of the usual critical exponent $y_K = 2$ (or $\sigma = -1/2$), see figure 11 obtained at $(A, x, c) = (4, 2, 0.2)$. Note that for those values the triple degeneracy conditions are not satisfied.

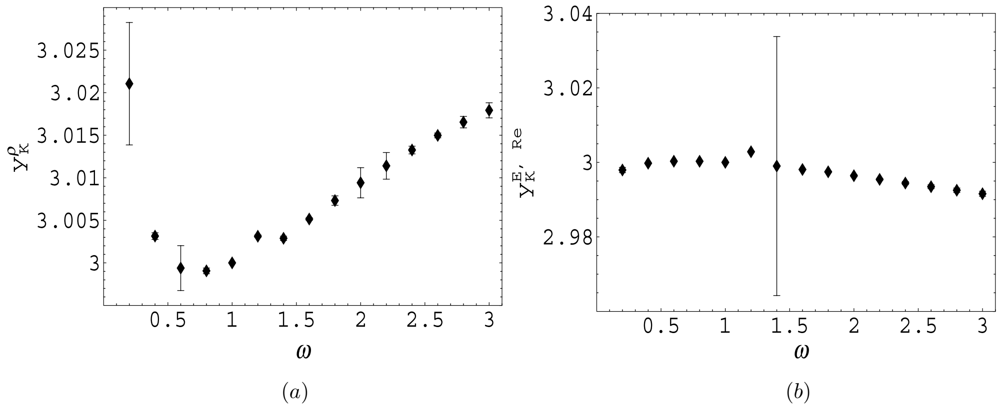

Figure 9. BST extrapolation for $0.2 \leqslant \omega \leqslant 3.0$ of y_Δ^ρ and y_Δ^E, (*a*) and (*b*) respectively. (*b*) The real part of the closest *b*-zeros have been used. The *b*-zeros are calculated at $c = 0.5$ while $x = 0.744\,681$ and $A = \sqrt{V(1-c^4)} \approx 2.004\,64$ are obtained from (43) and (44) respectively.

4.3. *c-zeros*

Now we investigate the possibility of having the Fisher zeros of the BEG model with a new critical behavior on the complex c-plane (complex Ising coupling J) with the other couplings H , Δ and K as real numbers. This is the most involved case since (31) and (32) depend on c in a complicated way. It is possible (see the appendix) to combine them and derive a quadratic equation for the ES c_E which leads to $\lambda_1 = \lambda_2 = \lambda_3$:

$$l_0 + l_1 c_E + l_2 c_E^2 = 0, \tag{45}$$

where $l_i = l_i(A, b, x)$, $i = 0, 1, 2$, are polynomials given in the appendix. In particular, $l_2(A, b, x)$ is a cubic polynomial in the variable $A = 2\cosh(\beta H)$. Whenever $l_2 \neq 0$, a c-independent necessary constraint for the triple degeneracy condition $\lambda_1 = \lambda_2 = \lambda_3$ can be derived (see the appendix):

$$G(A, b, x) = 0, \tag{46}$$

where the polynomial $G(A, b, x) = P_{12}(A, b, x) = \sum_{m=0}^{12} g_m\, x^m$ has complicated coefficients $g_m = g_m(A, b)$ given in the appendix. We have investigated $G(A, b, x)$ for some fixed values $b = b_j = j/10$ with $j = 1, 2, \ldots, 99, 100$. Since $A > 2$ and $x > 0$, it is convenient to introduce the variables $B = 1/A$ and $t = 1/x$. A 3D numerical plot reveals that $B^{12}\, G(1/B, b_j, x) > 0$ on the compact region: $0 < B < 1/2$; $0 < x < 1$. Similarly, it turns out that $B^{12} t^{12} G(1/B, b_j, 1/t) > 0$ in the complementary region $0 < B < 1/2$; $0 < t < 1$. See, e.g., figure 10 obtained for the Blume–Capel model $b = 1$. Thus, the constraint $G(A, b, x) = 0$ is never satisfied if $l_2 \neq 0$.

Now we are left with $l_2(A, b, x) = 0$. Since, see (A.3), $B^3 l_2(1/B, b, x) = 243\, x(2\, b^4 - 9\, x^2) + \sum_{j=1}^{3} f_j\, B^j$ where all $f_j < 0$, if $x > \sqrt{2}b^2/3$ the condition $l_2 = 0$ cannot be obeyed, so we have an upper limit $x_{\max} = \sqrt{2}b^2/3$. On the other hand, $B^3 l_2(1/B, b_j, x) = 0$ is a cubic equation for $B = B(b_j, x)$. It is easy to check that only one of the three roots is real. By substituting such root in the cubic equation for c which comes from replacing $c^4(A, b, x)$ from (31) in (32), altogether with $c = -l_0/l_1$ (from (45) at $l_2(A, b, x) = 0$), we have a function $H[B(b_j, x), b_j, x] \equiv H_j(x)$. A plot of $H_j(x)$ for $0 < x < x_{\max}$, see for instance figure 12, shows that $H_j(x) \neq 0$ for all values $j = 1, 2, \ldots, 99, 100$.

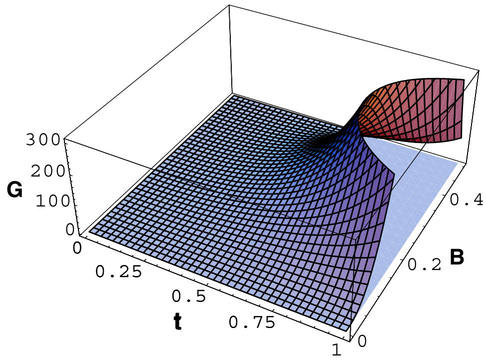

Figure 10. A 3D numerical plot of $G(1/B, b, 1/t) = 0$ at $b = 1$ on the compact region: $0 < B < 1/2$; $0 < t < 1$. The blue plane is $G(1/B, 1, 1/t) = 0$. The function $G(A, b, x)$ is given in the appendix, formula (A.6).

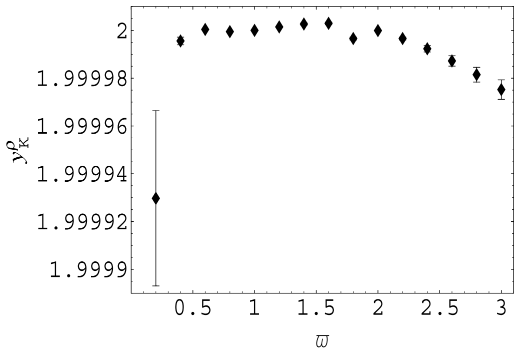

Figure 11. BST extrapolation of y_K^ρ for $0.2 \leqslant \omega \leqslant 3.0$ and $(A, x, c) = (4, 2, 0.2)$.

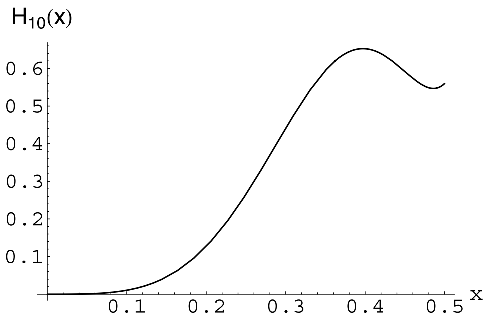

Figure 12. Plot of $H_{10}(x)$ $(b = 1)$ for $0 < x < x_{\max}$, where $x_{\max} = \sqrt{2}b^2/3 \approx 0.471\,405$.

In conclusion, we have not been able to find any Fisher's zero with new critical behavior $(\sigma = -2/3)$ by keeping the couplings (H, Δ) arbitrary real numbers and $\beta K_j = \ln(j/10)$ with $j = 1, 2, \ldots, 99, 100$. In particular, since $j = 10$ corresponds to the Blume–Capel model, we have a numerical proof that no such zeros show up in that model.

5. Conclusion

In section 2 we have studied the critical behavior of the linear density $\rho(z)$ of partition function zeros and established the usual result $\rho(z) \sim |z - z_E|^\sigma$ with $\sigma = -1/2$ ($y_z = 2$) about edge singularities z_E for an arbitrary three-state spin model that can be solved via a 3×3 transfer matrix. Our proof applies to all types of zeros associated with any of the couplings appearing in the spin model. Thus, generalizing the previous proof of $y_T = y_H = 2$ given in [9] for the Blume–Capel model. In particular, we have demonstrated how the universality of $\sigma = -1/2$ is related with a permutation symmetry of the two largest eigenvalues of the transfer matrix. Our results are in agreement with the conjecture made in [16] that $y_T = y_H$ holds in $d = 1, 2, 3$ dimensions. We have also shown that any violation of $\sigma = -1/2$ can only occur in special regions of the parameter space of the model. A new critical behavior with $\sigma = -2/3$ can occur where a triple degeneracy of transfer matrix eigenvalues takes place, though this is not a sufficient condition.

The case of the vanishing magnetic field ($H = 0$) in the BEG model is simpler and allowed a general analytic proof that $\sigma = -2/3$ requires a non-vanishing magnetic field ($H \neq 0$). We have shown, in subsection 4.1, that it is possible in both regions $K > 0$ and $K < 0$ to fine tune the couplings of the BEG model in order to find $\sigma = -2/3$ for x-zeros ($x = \mathrm{e}^{\beta\Lambda}$); however, this is never possible for the Blume–Capel model ($K = 0$). In subsection 4.2 we have also found b-zeros ($b = \mathrm{e}^{\beta K}$) with $\sigma = -2/3$.

The case of complex temperature zeros (Fisher's zeros or c-zeros, $c = \mathrm{e}^{-\beta J}$) is the most involved one (subsection 4.3). We have not been able to find any point in the three-dimensional space of real couplings (Δ, K, H) with $\sigma \neq -1/2$. In fact, for the Blume–Capel model ($K = 0$) we have proved that $\sigma = -2/3$ is not possible at Fisher edges as long as we keep H and Λ real numbers. For $K \neq 0$ our results for Fisher zeros are not conclusive and more research is needed. For completeness we mention (not displayed in this work) that we have found $\sigma = -2/3$ at Fisher edges if we allow some of the couplings (Δ, H, K) acquire complex values.

We believe that, see also [10, 22, 23], the universality of the new critical behavior $\sigma = -2/3$ at edge singularities of one-dimensional spin models with short-range interactions is well established now.

Furthermore, since the drop from $\sigma = -1/2$ down to $\sigma = -2/3$ is related to triple degeneracy of transfer matrix eigenvalues and the number of such eigenvalues is infinite for $d > 1$, we might speculate that an analogous change also occurs in higher-dimensional models ($d > 1$) under specific conditions. In particular, for $d = 2$ it could explain eventually the sudden drop from $\sigma = -0.15(2)$ (close to the usual critical value $-1/6$) for $49 \leqslant T \leqslant 53K$ down to $\sigma = -0.365$ at $T = 34K$, as indirectly measured in a sample of $FeCl_2$ ferromagnet, see [7].

Finally, another interesting result of this work, compared to previous ones, is the appearance of the new critical behavior $\sigma = -2/3$ at the closest edges to the positive real axis. If we recall that the exponent σ at the closest edges to $\mathbb{R}_+$ is related to the thermodynamic exponent δ via $\sigma = 1/\delta$ for real (physical) phase transitions, it is possible that the new critical behavior found here is related in higher-dimensional models to a tricritical point of physical systems.

Acknowledgments

DD is partially supported by CNPq and FLS is supported by CAPES. A discussion with N A Alves on the FSS relations for general zeros is gratefully acknowledged.

Appendix

Here we carry out some algebraic manipulations with the two triple degeneracy conditions (31) and (32) in order to obtain a c-independent relationship. First of all, from the first triple degeneracy condition (31), we have

$$c^4 = [b^2(3 - A^2) + Abxc - (3A + x)xc^2]/(3b^2) \tag{A.1}$$

$$\equiv P_2(c), \tag{A.2}$$

where we have defined the second-degree polynomial $P_2(c)$ as the right-hand side of (A.1). We can use $c^5 = c\,P_2(c)$ in the second triple degeneracy condition (32) and reduce it to a cubic equation $P_3(c) = 0$ from which we get $c^3 \equiv \tilde{P}_2(c)$. Using $P_2(c) - c\,\tilde{P}_2(c) \equiv \tilde{P}_3(c) = 0$ we have another cubic equation $\tilde{P}_3(c) = 0$. Combining $\tilde{P}_3(c) = 0$ and $P_3(c) = 0$ we get $l_0 + l_1\,c + l_2\,c^2 = 0$ with

$$\begin{aligned} l_2 = x(&8748b^4 + 17\,496Ab^2x + 3888Ab^4x - 486A^3b^4x + 8748\,A^2\,x^2 + 5832\,b^2x^2 \\ &+ 2430A^2b^2x^2 + 288\,A^2b^4x^2 + 5832Ax^3 + 2187A^3x^3 + 864Ab^2x^3 + 972x^4 \\ &+ 2025A^2x^4 + 624Ax^5 + 64x^6) \end{aligned} \tag{A.3}$$

$$\begin{aligned} l_1 = bx(&-972A^2b^4 + 81A^4b^4 - 7290Ab^2x + 486A^3b^2x - 192A^3b^4x - 2916A^2x^2 - 1296b^2x^2 \\ &- 540A^2b^2x^2 - 972Ax^3 - 729A^3x^3 - 432A^2x^4 - 64Ax^5) \end{aligned} \tag{A.4}$$

$$\begin{aligned} l_0 = b^2(&162A^3b^4 - 8748b^2x + 2916A^2b^2x + 162A^4b^2x + 36A^4b^4x - 8748Ax^2 \\ &+ 2916A^3x^2 - 1944Ab^2x^2 + 702A^3b^2x^2 - 2916x^3 - 1215A^2x^3 + 729A^4x^3 \\ &- 1296Ax^4 + 432A^3x^4 - 192x^5 + 64A^2x^5). \end{aligned} \tag{A.5}$$

If $l_2 \neq 0$ we can define the first-degree polynomial $P_1(c) = -(l_0 + l_1c)/l_2$. Using $c^3 = cP_1(c)$ we can reduce $P_3(c) = 0$ to a second-degree polynomial which combined with $c^2 = P_1(c)$ determines $c = c(A, b, x)$. Plugging it back in $l_0 + l_1c + l_2c^2$ we finally have a c-independent necessary condition for triple degeneracy of the transfer matrix eigenvalues:

$$G(A, b, x) = \sum_{m=0}^{12} g_m x^m = 0, \tag{A.6}$$

where $l_2 \neq 0$ and the reader can check the following coefficients:

$$g_0 = A^{12}b^{12}; \quad g_1 = 72A^9b^{10}(A^2 - 3); \quad g_2 = 108A^6b^8(108 - 90A^2 + 17A^4) \tag{A.7}$$

$$g_3 = 3A^5b^6(69\,984 - 44\,712A^2 + 7128A^4 - 36A^6 + 1728A^2b^2 - 696A^4b^2 + 67A^6b^2) \tag{A.8}$$

$$\begin{aligned} g_4 = 6A^4b^4(&262\,440 - 157\,464A^2 + 25\,758A^4 - 648A^6 - 23\,328b^2 + 29\,484A^2b^2 \\ &- 9693A^4b^2 + 951A^6b^2 - 8A^4b^4 + 2A^6b^4) \end{aligned} \tag{A.9}$$

$$\begin{aligned} g_5 = -9A^3b^2(&-629\,856 + 384\,912A^2 - 69\,984A^4 + 3240A^6 + 256\,608b^2 \\ &- 250\,776A^2b^2 + 78\,300A^4b^2 - 8397A^6b^2 + 117A^8b^2 \\ &+ 4608A^2b^4 - 2336A^4b^4 + 296A^6b^4) \end{aligned} \tag{A.10}$$

$$\begin{aligned} g_6 = 3A^2(&2834\,352 - 1889\,568A^2 + 419\,904A^4 - 34\,992A^6 + 972A^8 - 1889\,568b^2 \\ &+ 21\,17016A^2b^2 - 749\,412A^4b^2 + 95\,256A^6b^2 - 2646A^8b^2 + 186\,624b^4 \\ &- 285\,120A^2b^4 + 142\,884A^4b^4 - 29\,013A^6b^4 + 2050A^8b^4) \end{aligned} \tag{A.11}$$

$$g_7 = 3A(1889\,568 - 472\,392A^2 - 183\,708A^4 + 64\,152A^6 - 5508A^8 + 243A^{10} - 1399\,680b^2 + 769\,824A^2b^2 + 648A^4b^2 - 55\,782A^6b^2 + 7350A^8b^2 + 46\,080A^2b^4 - 36\,480A^4b^4 + 9568A^6b^4 - 832A^8b^4) \tag{A.12}$$

$$g_8 = 3(314\,928 + 332\,424A^2 - 251\,505A^4 + 57\,591A^6 - 8586A^8 + 873A^{10} - 248\,832b^2 - 93\,312A^2b^2 + 161\,856A^4b^2 - 47\,424A^6b^2 + 4170A^8b^2 + 256A^4b^4 - 128A^6b^4 + 16A^8b^4) \tag{A.13}$$

$$g_9 = A(279\,936 - 217\,728A^2 + 114\,156A^4 - 33\,489A^6 + 3547A^8 - 165\,888b^2 + 115\,200A^2b^2 - 26\,496A^4b^2 + 2016A^6b^2) \tag{A.14}$$

$$g_{10} = 3A^2(A^2-4)(8208 - 5028A^2 + 739A^4);\ g_{11} = 48A(A^2-4)^2(13A^2-48) \tag{A.15}$$

$$g_{12} = 64(A^2-4)^3. \tag{A.16}$$

References

[1] Yang C N and Lee T D 1952 *Phys. Rev.* **87** 404
Lee T D and Yang C N 1952 *Phys. Rev.* **87** 410
[2] Bena I, Droz M and Lipowski A 2005 *Int. J. Mod. Phys.* B **19** 4269
[3] Fisher M 1978 *Phys. Rev. Lett.* **40** 1610
[4] Cardy J L 1985 *Phys. Rev. Lett.* **54** 1354
[5] Matveev V and Schrock R 1996 *Phys. Rev.* E **53** 254
[6] Kim S-Y 2006 *Phys. Rev.* E **74** 011119
[7] Binek C 2003 *Ising-Type Antiferromagnets* (Berlin: Springer)
Binek C 1998 *Phys. Rev. Lett.* **81** 5644
[8] Glumac Z and Uzelac K 1994 *J. Phys. A: Math. Gen.* **27** 7709
[9] Ghulghazaryan R G, Sargsyan K G and Ananikian N S 2007 *Phys. Rev.* E **76** 021104
[10] Dalmazi D and Sá F L 2008 *Phys. Rev.* E **78** 031138
[11] Itzykson C, Pearson R B and Zuber J B 1983 *Nucl. Phys.* B **220** 415
[12] Kurze D A 1983 *J. Stat. Phys.* **30** 15
[13] Fisher M 1980 *Suppl. Progr. Theor. Phys.* **69** 14
[14] Wang X-Z and Kim J S 1998 *Phys. Rev.* E **58** 4174
[15] Fisher M E 1965 *Lectures in Theoretical Physics. Statistical Physics, Weak Interactions, Field Theory* Vol VIIC ed W E Brittin (Boulder, CO: University Press of Colorado)
[16] Kim S-Y 2002 *Nucl. Phys.* B **637** 409
[17] Kim S-Y 2008 *Nucl. Phys.* B **805** 441
[18] Matveev V and Schrock R 1996 *Phys. Lett.* A **215** 271
[19] Matveev V and Schrock R 2008 *J. Phys. A: Math. Theor.* **41** 135002
[20] Saarloos W van and Kurze D A 1984 *J. Phys. A: Math. Gen.* **17** 1301
[21] Biskup M, Borgs C, Chayes J T, Kleinwaks L J and Kotecky R 2000 *Phys. Rev. Lett.* **84** 4794
[22] Dalmazi D and Sá F L 2008 *J. Phys. A: Math. Theor.* **41** 505002
[23] Mittag L and Stephen M J 1984 *J. Stat. Phys.* **35** 303
[24] Blume M, Emery V J and Griffiths R B 1971 *Phys. Rev.* A **4** 1071
[25] Blume M 1966 *Phys. Rev.* **141** 517
Capel H W 1966 *Physica* **32** 966
[26] Lassettre E N and Howe J P 1941 *J. Chem. Phys.* **9** 747
[27] Ashkin J and Lamb W E 1943 *Phys. Rev.* **64** 159
[28] Almeida L A F and Dalmazi D 2005 *J. Phys. A: Math. Gen.* **38** 6863
[29] Creswick R J and Kim S-Y 1997 *Phys. Rev.* E **56** 2418
[30] Bulirsch R and Stoer J 1964 *Numer. Math.* **6** 413
[31] Henkel M and Schutz G 1988 *J. Phys. A: Math. Gen.* **21** 2617